



# Activated carbon doped WO<sub>3</sub> for photocatalytic degradation of rhodamine-B

Muhammad Bilal Tahir<sup>1</sup> · Maria Ashraf<sup>1</sup> · Muhammad Rafique<sup>1</sup> · Mohsin Ijaz<sup>1</sup> · Sohail Firman<sup>1</sup> · Iqra Mubeen<sup>1</sup>

Received: 23 July 2019 / Accepted: 19 August 2019 / Published online: 26 August 2019  
© King Abdulaziz City for Science and Technology 2019

## Abstract

In this research work, tungsten trioxide (WO<sub>3</sub>) and activated doped WO<sub>3</sub> composites were prepared for the photocatalytic degradation of rhodamine-B. Activated carbon was prepared by waste sugarcane burgesses, tungsten trioxide (WO<sub>3</sub>) was synthesized by precursor sodium tungstate dihydrate (Na<sub>2</sub>WO<sub>4</sub>·2H<sub>2</sub>O) using hydrothermal method. To study the morphology, functional groups, band gap, purity and optical properties of the prepared catalyst SEM, FTIR, PL and UV–Vis spectroscopy were used. SEM micrograph shows that tungsten trioxide has nanocubic rods-like structure with size 50–500 nm. Morphological results showed that nano rods become sharper when activated carbon were added in WO<sub>3</sub>. The average nanorods have average size 20–250 nm which is very efficient for degradation. UV–Vis spectroscopy shows that band gap of the fabricated catalyst changes from 2.76 to 2.26 eV by varying the concentration ratio of the activated carbon. FTIR analysis the functional groups of the prepared catalyst. PL-spectroscopy determined that the maximum excitation wavelength was 446 nm. Photocatalytic results show that 2% activated carbon doped WO<sub>3</sub> composite shows the maximum degradation rate as compare to the other prepared catalyst. Synthesized catalysts are environment friendly, cost effective and due to low band gap very useful for the degradation purpose.

**Keywords** Activated carbon · Tungsten trioxide · Photocatalytic degradation · Hydrothermal process

## Introduction

As the population of the world is increasing, the demand of people also rising which indirectly causes the environmental pollution in the world. Water pollution is a type of environmental pollution which has become the major problem in the whole world. Almost 50% people of the world have shortage of fresh and clean water. The need of the hour is to save more water according to needs as it is considered the essential element for the proper functioning of the ecosystem. Water contains many pollutants but in aquatic environment the most common pollutants are dyes which are harmful due to their toxicity. Industries manufacture dyes at large scale which are used in medicals, leather, fabrics, cosmetics and paper industries at large scale. The annual production

of dyes for the industry is about 10<sup>6</sup> with over 7 × 10<sup>5</sup> tones. The waste water of the industries contains more than 15% of the dyes which are harmful for civil and aquatic life (Anfar et al. 2018). The dyes are classified as anionic dyes, non-ionic dyes and cationic dyes. Rhodamine-B is widely used in printing and as a colorant in food items and textile industries which is very dangerous for human health, plants and animals. Many diseases such as irritation in humans' skin, eyes and cancer are due to excessive use of rhodamine-B (Chaudhary et al. 2017).

International community has great concern in this matter as everyone wants to solve this problem (Matthews 1990). The work over the removal of dyes is due to their toxicity, so researchers have introduced many methods to remove dyes from wastewater and convert it into less harmful. But there is no specific method which removes all type of compounds and dyes from industrial waste water (Tahir et al. 2018). Current physical methods which are used for the removal of waste from the water are filtration, ion exchange, reverse osmosis and distillation which are only suitable for inorganic compounds (Andreozzi et al. 1999). To remove the organic waste compound from water chemical oxidation process has

✉ Muhammad Bilal Tahir  
m.bilaltahir@uog.edu.pk

✉ Mohsin Ijaz  
mohsin@live.no

<sup>1</sup> Department of Physics, Faculty of Sciences, University of Gujrat, Hafiz Hayat Campus, Gujrat 50700, Pakistan

become one of the best physiochemical process. It converts toxic organic molecules into carbon dioxide, sulfates, and nitrates using highly oxidizing reagents.

More valuable advance oxidizing processes are radiolysis, sonolysis, ozonolysis, photo-femto reaction and photocatalysis. But the most suitable and low-cost method for the dyes degradation is photocatalysis. In recent years, various voluminous literatures are present to improve the photocatalytic process for the dyes degradation of industrial wastewater (Pera-Titus et al. 2004). Photo-catalysis is an effective advanced oxidation process that can be used in the purification of toxic and harmful dyes. Using this approach dyes degradation can be done in the presence of catalyst under visible light without adding any oxidizing agent as a second harmful pollutant (Esplugas et al. 2002). Semiconductor photo-catalysts for purification of water from inorganic materials is consider as a valuable method. The best advantage of photocatalyst was that they are insoluble in water and can be used again (Klavarioti et al. 2009).

Many materials have been used for the removal of rhodamine-B from wastewater by iron-based nanoparticles. TiO<sub>2</sub> nano material is doped with metal for the purification of water, is also used. In this research work, tungsten trioxide is used for the removal of rhodamine-B. It has been reported that the tungsten trioxides WO<sub>3</sub> is a n-type semiconductor having indirect band gap 2.7 eV. This semiconductor is one of best transition metal oxides it exists in many forms such as nanowires, nano belts and nanorods. WO<sub>3</sub> is used for the removal of organic pollutants due to its stable physical and chemical properties and also its high absorption capacity of visible light. Pure tungsten trioxide has lower energy conversion efficiency which can be increased by doping. Its nano structure is cubic when other material is added in it then its band gap reduces. For the electro chromic performance, structure of WO<sub>3</sub> is also very important (Oller et al. 2011).

There are many methods to synthesis the tungsten trioxide such as sol-Gel method, electrode position method, electro chemical ionization method and hydrothermal method. But hydrothermal method is low in cost, environment friendly and the energy losses are less in it (Hepel and Hazelton 2005).

Activated Carbon is basic form of carbon which has small size and low volume pores. It has large surface area 1 g of AC contain 3000 m<sup>2</sup> surface area for the chemical reaction. Its micro porosity is very high (Cao et al. 2011). AC in laboratories is also used for the purification and filtration of water. In the rayon fiber technique, activated carbon is used to filter the materials by forming the carbon cloth filter (Luo and Hepel 2001). Present research work is based on analysis of photo-catalytic efficiency of the fabricated samples for the dyes degradation (Amin 2008). Rhodamine-B dye was used in the photocatalytic reactor, it has been noticed that pure WO<sub>3</sub> and activated carbon doped WO<sub>3</sub> composites were

really promising photocatalysts for the degradation under visible light (Krishnan and Anirudhan 2002).

## Material and method

In this research study, the material used for the preparation of catalysts are, sodium tungstate dihydrate (Na<sub>2</sub>WO<sub>4</sub>·2H<sub>2</sub>O) 2 g, sodium chloride (NaCl) 3 g, sulphuric acid (H<sub>2</sub>SO<sub>4</sub>) 20 ml, hydrochloric acid (HCl) 10 ml, distill water 100 ml, ethanol 5 ml, sugarcane borges powder about 50 g and rhodamine-B.

### Preparation of activated carbon (AC)

Waste sugarcane borgeses (SCB) were collected from the sugarcane juices shop. These borgeses were washed two to three times with normal tap water and dried in the sun light for 2 days. Brown and white borgeses separated, then grinded in the big grander machine (Ito et al. 2008). 10 ml H<sub>2</sub>SO<sub>4</sub> was added in the SCB powder and dried these samples in oven for 20 h at 250 °C for the complete reaction (Lv et al. 2011). Then prepared sample was washed until its pH reached to 7 and grinded again. Pure form of AC was obtained after that process the complete process is shown in Fig. 1 which were got time to time.

### Preparation of nanoparticles of Tungsten trioxide WO<sub>3</sub>

For tungsten trioxide sodium tungstate dehydrate (Na<sub>2</sub>WO<sub>4</sub>·2H<sub>2</sub>O) 1.067 g and pure sodium chloride (NaCl) about 0.038 g, were added in 20 ml of distill water. The solution was Starrier for 20 min at 300 rpm and during starrier 5 ml hydrochloric acid was added in the solution drop wise (Pihosh et al. 2014). Then the color of the sample was changed from white to light yellow which indicated the accuracy of the samples as shown in Fig. 2.

Stainless steel autoclave was used for the hydrothermal process, prepared solution was added in the Teflon bottle and was placed into the oven for 24 h at 150 °C temperature. When the reaction times completed the autoclave was placed to cool down at the normal temperature for 2 h. Then this sample was washed 3 to 5 time by distilled water till its pH reached to 7. Sample was placed in the china dish, for 5 min about 550 °C temperature. Dried pure WO<sub>3</sub> sample were collected by help of spatula.

### Synthesis of activated carbon doped WO<sub>3</sub> composites

For the synthesis of activated carbon doped WO<sub>3</sub> composites, first added 5 ml of ethanol in 0.01 g of activated carbon



**Fig. 1** Grinding process of dry sugarcane bursesses

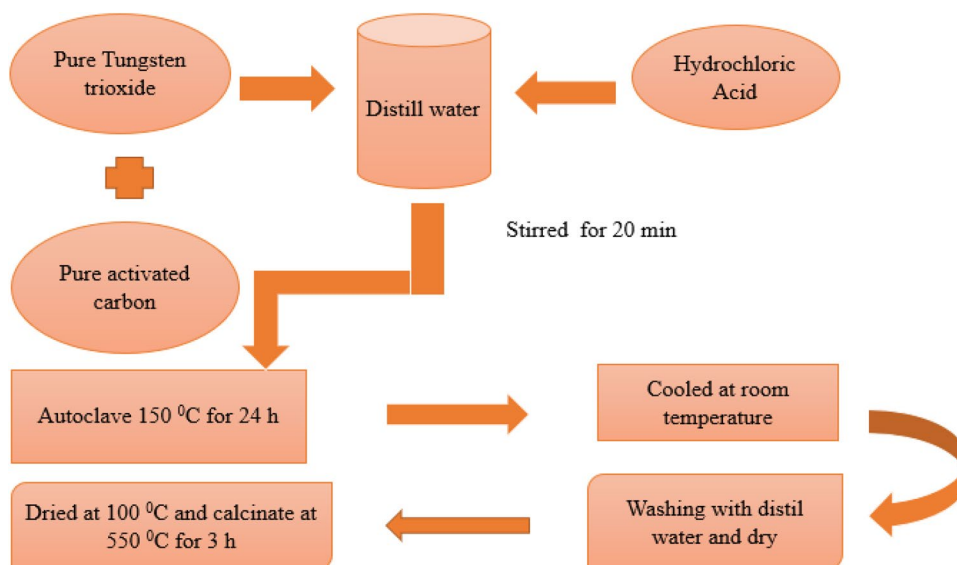


**Fig. 2** Procedure for synthesis of  $\text{WO}_3$

and sonicated it for 10 min. 1 g of pure  $\text{WO}_3$  and prepared activated carbon were added in 10 ml distilled water. Solution had been stirred continuously at 300 rpm for 20 min in the dark room, during this process 5 ml hydrochloric acid was added drop wise. Solution saw placed in the autoclave at 150 °C temperature for 24 h (Zhang et al. 2013). 1%

activated carbon doped  $\text{WO}_3$  was gained after washing and drying. For the 2% of AC doped  $\text{WO}_3$  composite, 0.02 g was taken in the same percentage of  $\text{WO}_3$  and the same procedure was repeated. Flow chart in Fig. 3 clarifies the procedure of the preparation of activated carbon doped  $\text{WO}_3$  composites.

**Fig. 3** Flow chart for the synthesis of activated carbon doped  $\text{WO}_3$  composites



### Characterization techniques

Pure  $\text{WO}_3$  and its activated carbon doped composites nanoparticles were characterized by the characterization techniques such as scanning electron microscopy (SEM), Fourier transformation infra-red spectroscopy (FTIR), UV–Vis spectroscopy, and photoluminescence spectroscopy (PL) (Kim et al. 2012). To study the morphology, functional groups, band gap and optical properties of the synthesis samples.

## Results and discussion

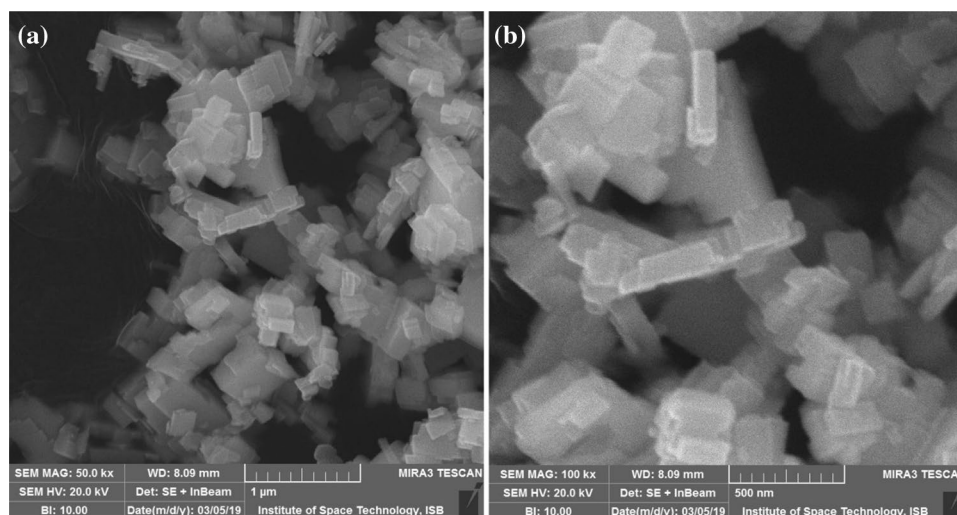
### SEM result analysis

To study the morphology and size of the samples with the help of analytic picture scanning electron microscopy

(Hitachi TM-1000) was used (Alaei et al. 2012). Activated carbon doped  $\text{WO}_3$  and pure  $\text{WO}_3$  nanoparticles results showed that these samples had shapes such as nanorods having the 20–250 nm range, their size, length and diameter range were varying as we changed the concentration ratio of the activated carbon (Montes-Burgos et al. 2010). Micrograph of pure  $\text{WO}_3$  of the SEM and its activated carbon coupled samples shown in Fig. 4. The band gap energy of pure tungsten oxide is large and changed inversely as the content ratio of activated carbon was changed. Each single crystal of tungsten oxide take growth from nucleus and grow continue in all directions (Helfrich et al. 2006).

In the first early stage, sodium tungstate dehydrate and hydrochloric acid started reacting and ions formed, thereafter nucleation growth started. These ions reacted very festally to form the nuclei of  $\text{WO}_3$  ( $\text{H}_2\text{O}$ ). Thermodynamic parameters changed the nucleation growth, particle size, size

**Fig. 4** SEM results of pure  $\text{WO}_3$



of nuclei, which depends upon the super-saturation. It had been analysis that the value of pH of the solution played an important role in the formation of morphology (Willard et al. 2004). Presence of AC in pure  $\text{WO}_3$  changed the orientation of the nanorods in all the directions as shown in Fig. 5.

Micrograph of SEM clearly indicated that activated carbon nanoparticles intertid with the pure tungsten trioxide.  $\text{WO}_3$  SEM result showed that its nanoparticle had size 78–128 nm but when activated carbon 2% content ratio were added in the tungsten trioxide its size was reduced from 50 to 102 nm and the nanorods became sharper (Hole et al. 2013). By SEM results observation it was cleared that if we access the doping of AC in pure  $\text{WO}_3$  then its size also changes (Adhikari et al. 2014). Figure 5 shows critical pictures of the SEM of activated carbon doped  $\text{WO}_3$  composite with different magnification ranges.

### Analysis of Fourier transform-infrared spectroscopic result

Wave numbers ( $\text{cm}^{-1}$ ) and functional group that are found in the material were determined by FTIR spectrometer. Infrared spectroscopic graph of activated carbon had a lot of adsorption wave numbers (Paramasivam et al. 2010). Its highest adsorption frequency was observed at  $3035.05 \text{ cm}^{-1}$  which is due to bonded  $-\text{OH}$  groups, the adsorption at  $2109.06 \text{ cm}^{-1}$  was due to the  $\text{C}=\text{C}$  stretching vibrational frequency and the lowest adsorption frequency at  $1156.81 \text{ cm}^{-1}$  was due to the  $\text{C}-\text{O}-\text{C}$  stretching vibration (Kim et al. 2010). FTIR spectroscopic graph of activated carbon is shown in Fig. 6.

FTIR spectrum result for  $\text{WO}_3$  and AC doped  $\text{WO}_3$  had the various adsorption bands (Abazari et al. 2014). The highest adsorption was obtained at  $3442.5 \text{ cm}^{-1}$  due to surface symmetric vibration that was formed because of  $\text{O}-\text{H}$  banding with crystal structure which was generated due to

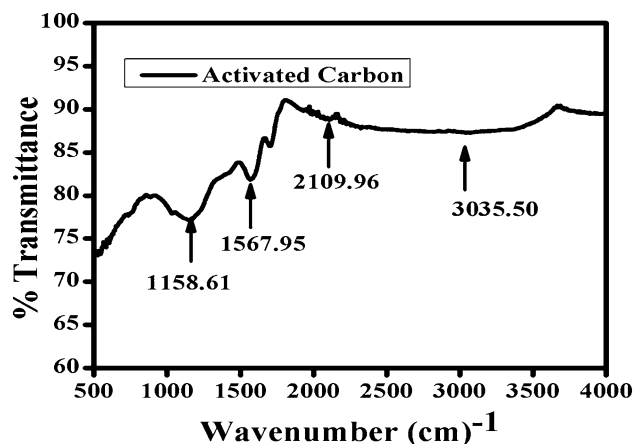


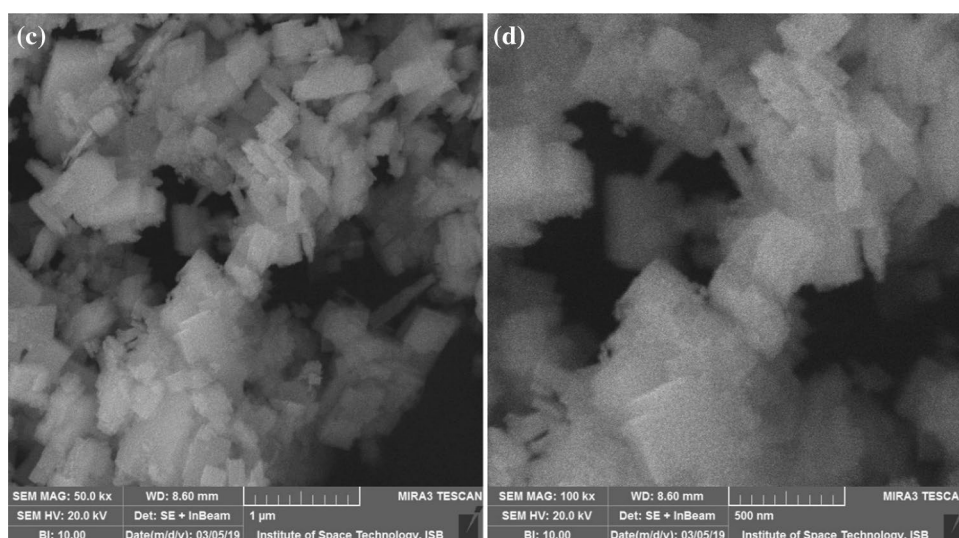
Fig. 6 FTIR spectrum result of activated carbon nano particles

hydrothermal preparation way (Sudrajat and Babel 2016). The adsorption at  $804.14 \text{ cm}^{-1}$  was the lower frequency peak which was owing to  $\text{CH}$  band out of phase deformation and the band adsorption at  $1649.02 \text{ cm}^{-1}$  were due to the stretching vibration of amino group as shown in Fig. 7. The adsorption at  $615.88 \text{ cm}^{-1}$  was due to the  $\text{C}-\text{O}-\text{H}$  twist broad. When activated carbon was added in the pure  $\text{WO}_3$  then absorption rate of tungsten trioxide was changed (Vinodgopal et al. 1996). 1% activated carbon had small change in absorption rate but when 2% of AC was added in  $\text{WO}_3$ , FTIR spectrum graph showed that change in absorption rate was higher.

### UV-Vis spectroscopy to measure band gap

The UV-visible spectrometer (UV-Vis absorption: TU-1901) was used to determine the UV-Vis spectrum of pure  $\text{WO}_3$  and activated carbon doped  $\text{WO}_3$  composites.

Fig. 5 SEM results of AC/ $\text{WO}_3$  particles at  $\mu\text{m}$  and  $\text{nm}$  scale



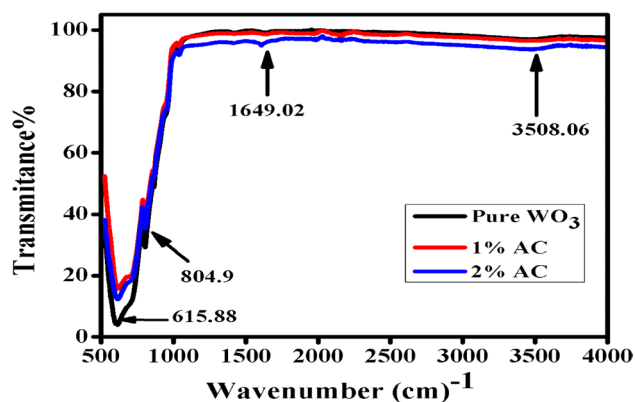


**Fig. 7** FTIR spectrum results of pure  $\text{WO}_3$  and activated carbon doped  $\text{WO}_3$  composites

These materials concerned with optical band gap and defects which depend upon on the absorbance (Cai et al. 2015).

The band gap measured from tauc plot were 2.76 eV for pure  $\text{WO}_3$ , 2.42 and 2.26 eV were determined by 1% AC composite, and 2% AC composite, respectively, as shown in Fig. 8. The reduction in the band gap when we added 1% and 2% activated carbon in  $\text{WO}_3$  clearly shows that the doping of AC in the lattice of  $\text{WO}_3$ . It also changes the phases of the tungsten trioxide nano particles. This is due to the increase in doping concentration which changes the stimulation and excitation of the electron from valance band to conduction band.

It has been noticed that difference in band gap between pure  $\text{WO}_3$  and activated carbon doped  $\text{WO}_3$  is owing to the electronic coupling and perfect interstitial packing of the nano particles.

### Photoluminescence measurements

To determine the defects produced in the samples, photoluminescence spectroscopy (PL: RAMANLOG 6, UOG) had been utilized (Gan et al. 2016). The wavelength of the activated carbon doped  $\text{WO}_3$  composites are very important in the formation of energy, position, peaks and the intensity on the PL spectrum (Ding et al. 2017). At room temperature fabricated  $\text{WO}_3$  has maximum wavelength 446 nm which gradually decreases by increasing the concentration of the activated carbon in  $\text{WO}_3$  as shown in the Fig. 9. The first wavelength peak gives us band gap 2.78 eV which is accurate for tungsten trioxide. And second peak give us information of the impurities present in the samples.

### Photocatalytic activity for the degradation Rh-B

Homemade photocatalytic reactor having 400 W power metal halide lamp, was used to investigate the dye

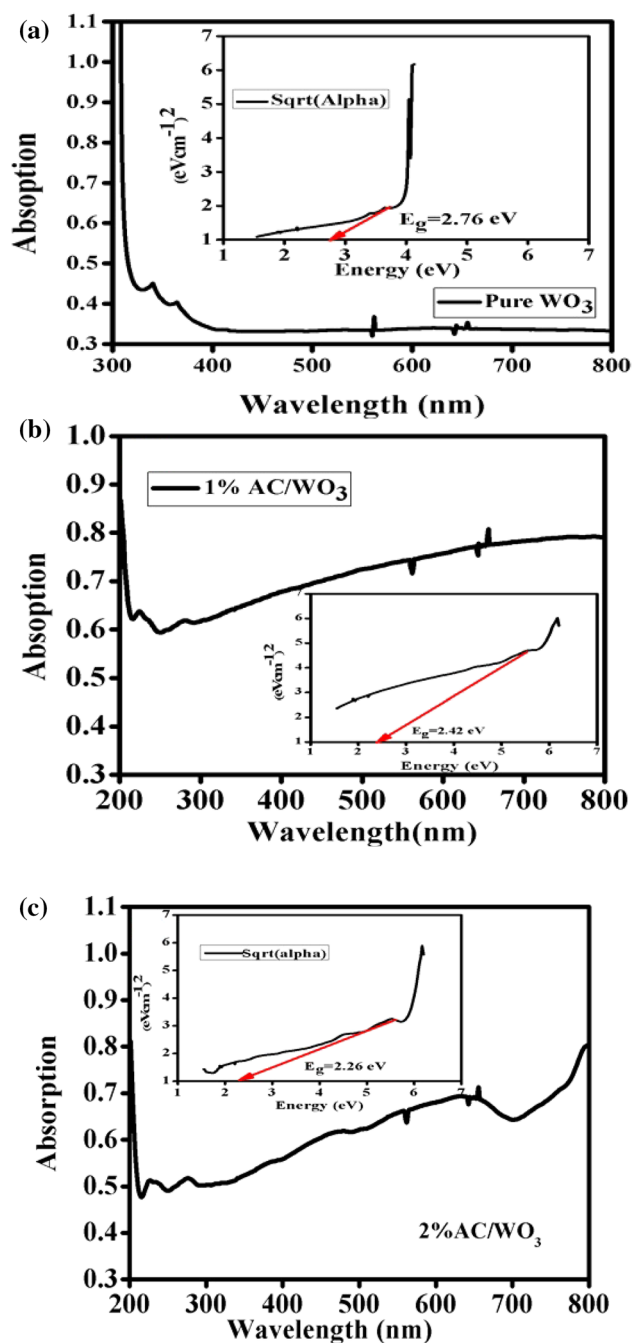


**Fig. 8** UV–Vis absorption spectrum of **a** pure  $\text{WO}_3$  **b** 1% AC doped  $\text{WO}_3$  **c** 2% AC doped  $\text{WO}_3$

degradation efficiency of the prepared samples.  $\text{WO}_3$  were considered really an efficient catalyst for the photo-catalytic activity (Ren et al. 2014). In 100 ml distill water 0.1 mg of rhodamine-B (Rh-B) dye was put and stirred in dark room for 30 min then 0.01 g of pure  $\text{WO}_3$  catalyst was added. Solution was placed in the reactor and after every 30 min 5 ml was taken from the solution, then getting UV–Vis spectrum, repeated this process for 180 min. Repeated same steps

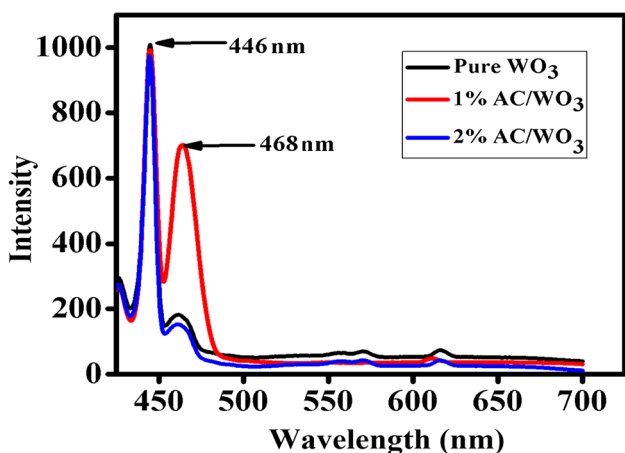


Fig. 9 PL-emission spectrum of pure WO<sub>3</sub> and its composites with AC

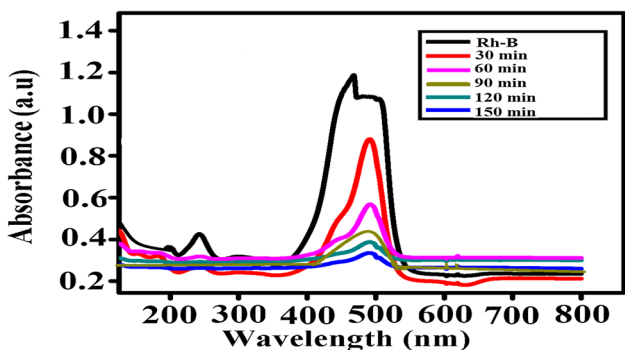


Fig. 10 Photo catalytic activity UV-Vis spectra of pure WO<sub>3</sub>

for activated carbon doped composite. To calculate the percentage degradation efficiency of those prepared catalysts following formula had been used:

$$\text{Degradation (\%)} = (1 - C/C_0) \times 100\%.$$

Here, initial concentration is  $C_0$  and after time  $t$ ,  $C$  is the concentration of dye. Figure 10 represents the UV-Vis spectra of Rh-B, absorption peak moves downward as soon as time interval is changed, this was the evidence of degradation of Rh-B with time (Hunge et al. 2018). From Figs. 11 and 12 it has been noticed that the degradation efficiency enhanced with increase in AC doped WO<sub>3</sub> composites and moved toward the visible range of light due to decrease in the band gap of the synthesis composites.

Increases the concentration ratio of activated carbon in the pure tungsten trioxide degradation efficiency were also increased. 1% activated carbon atoms doped in WO<sub>3</sub> nanoparticles gave the 63% degradation rate within the visible range.

2% activated carbon doped WO<sub>3</sub> degraded 76% Rh-B dye in 180 min which saw the evidence that its efficiency was

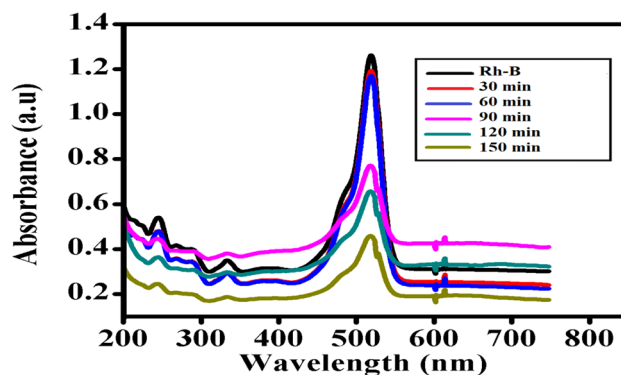


Fig. 11 Photo catalytic activity UV-Vis spectra of 1% activated carbon doped WO<sub>3</sub>

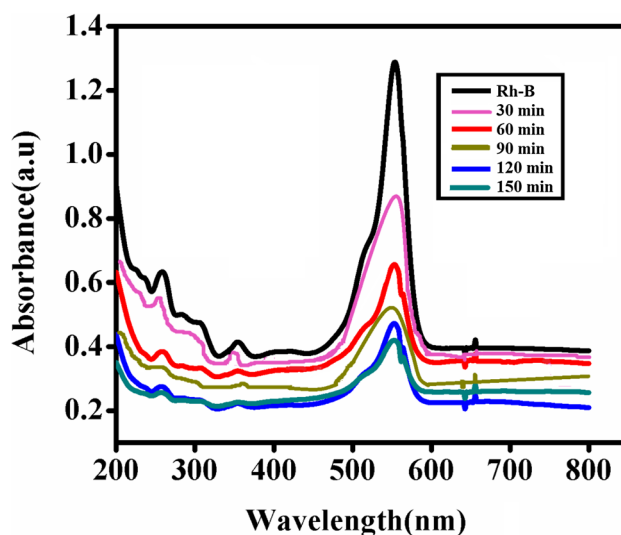
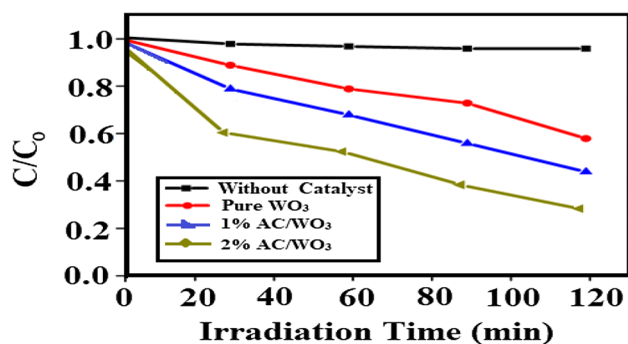


Fig. 12 Photo catalytic activity UV-Vis spectra of 2% activated carbon doped WO<sub>3</sub>

high as compare to all other composite materials. From the above figures, it was observed that degradation rate directly associated with the exposure time (El-Salamony et al. 2018). The highest degradation efficiency was observed for 2% AC doped WO<sub>3</sub> composite in the comparison of other composite materials.

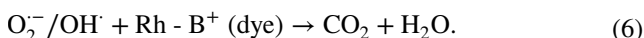
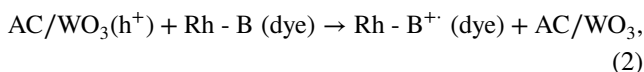
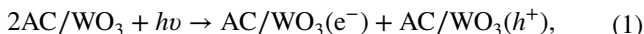
Figure 13 shows the photocatalytic concentration efficiency for degradation of Rh-B. It was observed that exposure time were directly proportion with the concentration rate. As concentration ratio decreases, the degradation intensity increased. The highest efficiency of the photo-catalyst was observed for composite having 2% AC as compare to the other samples.

In the photocatalytic activity when light with threshold frequency falls on the photocatalyst, the valance band electrons get excited. These electrons move toward the



**Fig. 13** Photocatalytic activity of WO<sub>3</sub> and activated carbon doped WO<sub>3</sub> composites

conduction band and the same numbers of holes are produced in the valence band (Yu et al. 2009). The WO<sub>3</sub> ions absorb the photo generation electrons and superoxide radicals are produced, in this way WO<sub>3</sub> works like a scavenger and reduces electron holes' recombination rate.



The hydroxyl radicals and hydrogen ions form when AC/WO<sub>3</sub> catalyst reacted with water (Yin et al. 2009). The holes combine with the Rh-B dye and charged it positively. When oxygen O<sub>2</sub> and electron reacted, the superoxide anion radical was produced (He et al. 2009). Both these hydroxyl ions and radical reacted then formed peroxide radicals and hydrogen ion. The superoxide anion and hydroxyl radicals formed strong oxidants which reacted with Rh-B and converted into CO<sub>2</sub> and water. The schematic diagram of photocatalysis degradation mechanism is given in Fig. 14.

## Conclusions

Photocatalytic method is really an efficient method to remove toxic dyes from the industrial waste water. This method always requires those catalysts which have low band gap energy. Characterization of the synthesis samples also proves that adding impurity in pure metal oxide material reduces its band gap and its degradation ability gradually increases. Hydrothermal method was also a unique method

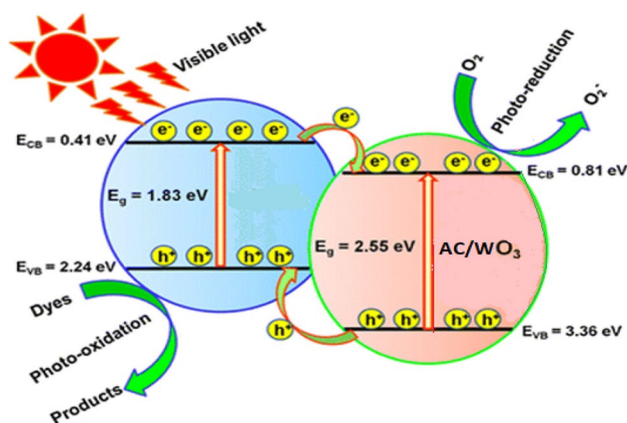


**Fig. 14** Photocatalysis mechanism of WO<sub>3</sub> and activated carbon doped WO<sub>3</sub> composites

for the preparation of pure WO<sub>3</sub> and its 1% and 2% activated carbon doped WO<sub>3</sub> composites. By examining the Rh-B dye, degradation was also verified that these catalysts have great efficiency. Measured band gap of WO<sub>3</sub> was 2.78 eV and activated carbon doped WO<sub>3</sub> composites show 2.42 eV and 2.26 eV. This is a great achievement which plays vital role in degradation process.

## Compliance with ethical standards

**Conflict of interest** On behalf of all authors, the corresponding author states that there is no conflict of interest.

## References

- Abazari R et al (2014) Characterization and optical properties of spherical WO<sub>3</sub> nanoparticles synthesized via the reverse microemulsion process and their photocatalytic behavior. *Mater Lett* 133:208–211
- Adhikari S, Sarkar D, Maiti HS (2014) Synthesis and characterization of WO<sub>3</sub> spherical nanoparticles and nanorods. *Mater Res Bull* 49:325–330
- Alaei M, Mahjoub AR, Rashidi A (2012) Effect of WO<sub>3</sub> nanoparticles on congo red and rhodamine B photo degradation. *Iran J Chem Chem Eng (IJCCE)* 31(1):23–29
- Amin NK (2008) Removal of reactive dye from aqueous solutions by adsorption onto activated carbons prepared from sugarcane bagasse pith. *Desalination* 223(1–3):152–161
- Andreozzi R et al (1999) Advanced oxidation processes (AOP) for water purification and recovery. *Catal Today* 53(1):51–59
- Anfar Z et al (2018) Well-designed WO<sub>3</sub>/activated carbon composite for rhodamine B removal: synthesis, characterization, and modeling using response surface methodology. *Fuller Nanotubes Carbon Nanostruct* 26(6):389–397
- Cai L et al (2015) Highly effective and stable Ag<sub>3</sub>PO<sub>4</sub>-WO<sub>3</sub>/MWCNTs photocatalysts for simultaneous Cr(VI) reduction and orange II degradation under visible light irradiation. *Appl Surf Sci* 353:939–948
- Cao J et al (2011) Photocatalytic activity of novel AgBr/WO<sub>3</sub> composite photocatalyst under visible light irradiation for methyl orange degradation. *J Hazard Mater* 190(1–3):700–706



- Chaudhary A et al (2017) TiO<sub>2</sub>, WO<sub>3</sub>, and V<sub>2</sub>O<sub>5</sub>, supported on activated carbon: preparation, structural and catalytic behaviour in photocatalytic treatment of phenol and lignin from olive mill wastewater. *Fresenius Environ Bull* 26(5):3529–3541
- Ding J et al (2017) Synergistic effects of electronic structure of WO<sub>3</sub> nanorods with the dominant 001 exposed facets combined with silver size-dependent on the visible-light photocatalytic activity. *Appl Catal B* 203:335–342
- El-Salamony RA et al (2018) Visible light sensitive activated carbon-metal oxide (TiO<sub>2</sub>, WO<sub>3</sub>, NiO, and SnO) nano-catalysts for photo-degradation of methylene blue: a comparative study. *Toxicol Environ Chem* 100(2):143–156
- Esplugas S et al (2002) Comparison of different advanced oxidation processes for phenol degradation. *Water Res* 36(4):1034–1042
- Gan L et al (2016) Visible light induced methylene blue dye degradation photo-catalyzed by WO<sub>3</sub>/graphene nanocomposites and the mechanism. *Ceram Int* 42(14):15235–15241
- He Z et al (2009) Photocatalytic degradation of rhodamine B by Bi<sub>2</sub>WO<sub>6</sub> with electron accepting agent under microwave irradiation: mechanism and pathway. *J Hazard Mater* 162(2–3):1477–1486
- Helfrich A, Brüchert W, Bettmer J (2006) Size characterisation of Au nanoparticles by ICP–MS coupling techniques. *J Anal Atom Spectrom* 21(4):431–434
- Hepel M, Hazelton S (2005) Photoelectrocatalytic degradation of diazo dyes on nanostructured WO<sub>3</sub> electrodes. *Electrochim Acta* 50(25–26):5278–5291
- Hole P et al (2013) Interlaboratory comparison of size measurements on nanoparticles using nanoparticle tracking analysis (NTA). *J Nanopart Res* 15(12):2101
- Hunge Y et al (2018) Degradation of organic dyes using spray deposited nanocrystalline stratified WO<sub>3</sub>/TiO<sub>2</sub> photoelectrodes under sunlight illumination. *Opt Mater* 76:260–270
- Ito S et al (2008) Fabrication of thin film dye sensitized solar cells with solar to electric power conversion efficiency over 10%. *Thin Solid Films* 516(14):4613–4619
- Kim J, Lee CW, Choi W (2010) Platinized WO<sub>3</sub> as an environmental photocatalyst that generates OH radicals under visible light. *Environ Sci Technol* 44(17):6849–6854
- Kim JK et al (2012) Inverse opal tungsten trioxide films with mesoporous skeletons: synthesis and photoelectrochemical responses. *Chem Commun* 48(98):11939–11941
- Klavarioti M, Mantzavinos D, Kassinos D (2009) Removal of residual pharmaceuticals from aqueous systems by advanced oxidation processes. *Environ Int* 35(2):402–417
- Krishnan KA, Anirudhan T (2002) Uptake of heavy metals in batch systems by sulfurized steam activated carbon prepared from sugarcane bagasse pith. *Ind Eng Chem Res* 41(20):5085–5093
- Luo J, Hepel M (2001) Photoelectrochemical degradation of naphthol blue black diazo dye on WO<sub>3</sub> film electrode. *Electrochim Acta* 46(19):2913–2922
- Lv K et al (2011) Synthesis and photo-degradation application of WO<sub>3</sub>/TiO<sub>2</sub> hollow spheres. *J Hazard Mater* 189(1–2):329–335
- Matthews RW (1990) Purification of water with near-UV illuminated suspensions of titanium dioxide. *Water Res* 24(5):653–660
- Montes-Burgos I et al (2010) Characterisation of nanoparticle size and state prior to nanotoxicological studies. *J Nanopart Res* 12(1):47–53
- Oller I, Malato S, Sánchez-Pérez J (2011) Combination of advanced oxidation processes and biological treatments for wastewater decontamination—a review. *Sci Total Environ* 409(20):4141–4166
- Paramasivam I et al (2010) WO<sub>3</sub>/TiO<sub>2</sub> nanotubes with strongly enhanced photocatalytic activity. *Chem A Eur J* 16(30):8993–8997
- Pera-Titus M et al (2004) Degradation of chlorophenols by means of advanced oxidation processes: a general review. *Appl Catal B* 47(4):219–256
- Pihosh Y et al (2014) Nanostructured WO<sub>3</sub>/BiVO<sub>4</sub> photoanodes for efficient photoelectrochemical water splitting. *Small* 10(18):3692–3699
- Ren H-T et al (2014) Improved photochemical reactivities of Ag<sub>2</sub>O/g-C<sub>3</sub>N<sub>4</sub> in phenol degradation under UV and visible light. *Ind Eng Chem Res* 53(45):17645–17653
- Sudrajat H, Babel S (2016) An innovative solar photoactive system N-WO<sub>3</sub>@ polyester fabric for degradation of amaranth in a thin-film fixed-bed reactor. *Sol Energy Mater Sol Cells* 149:294–303
- Tahir MB, Nabi G, Hassan A, Iqbal T, Kiran H, Majid A (2018) Morphology tailored synthesis of C-WO<sub>3</sub> nanostructures and its photocatalytic application. *J Inorg Organomet Polym Mater* 28(3):738–745
- Vinodgopal K, Wynkoop DE, Kamat PV (1996) Environmental photochemistry on semiconductor surfaces: photosensitized degradation of a textile azo dye, acid orange 7, on TiO<sub>2</sub> particles using visible light. *Environ Sci Technol* 30(5):1660–1666
- Willard M et al (2004) Chemically prepared magnetic nanoparticles. *Int Mater Rev* 49(3–4):125–170
- Yin M et al (2009) Mechanism investigation of visible light-induced degradation in a heterogeneous TiO<sub>2</sub>/eosin Y/rhodamine B system. *Environ Sci Technol* 43(21):8361–8366
- Yu K et al (2009) Visible light-driven photocatalytic degradation of rhodamine B over NaBiO<sub>3</sub>: pathways and mechanism. *J Phys Chem A* 113(37):10024–10032
- Zhang J et al (2013) Ultra-thin WO<sub>3</sub> nanorod embedded polyaniline composite thin film: synthesis and electrochromic characteristics. *Sol Energy Mater Sol Cells* 114:31–37